

*EVS30 Symposium
Stuttgart, Germany, October 9 - 11, 2017*

Intelligent photovoltaic-grid system for electric vehicles charging station

A. HASSOUNE^{1, 2}, M. KHAFALLAH¹, A. MESBAHI¹, D. BREUIL²

¹*Laboratory of Energy & Electrical Systems (LESE)*

Hassan II University of Casablanca, ENSEM, Casablanca, Morocco

a.hassoune@IEEE.org, m.khafallah@gmail.com, abdelouahed.mesbahi@gmail.com

²*Laboratoire Energie Renouvelable Propre Alternative (LERPA)*

EIGSI La Rochelle, France

dominique.breuil@eigsi.fr

Summary

This work focuses on a smart algorithm to optimize energy in electric vehicles charging station while considering numerous constraints as the inefficiency of renewable energy sources and also the potential limited power given by the grid. However, the PV is considered a primordial source to feed the storage system, directly tied into a voltage DC link, the lithium-ion battery is implemented in this platform to complete the power flow of each potential charging scenario. The management algorithm is taking into account the fluctuant power state of both the DC and the AC link, and it treats the SOC of batteries.

1 Introduction

The environmental challenges and the predicted shortage of fossil fuels have made electric vehicles (EVs) more involved in mobility. Yet, their development at a wider scale faces specific barriers amongst with EVs charging time is a major inconvenient for consumers [1]. On another hand, the increase of renewable energy sources (RES) integration in electrical systems, opens the way for combining PV sources with grid supply. This requires to implement a buffer battery [2], in order to store the renewable energy and/or to decrease the power peak when rapid charging is operating. Multiple considerations intend to enhance the reliability of system by reducing the power burden on the distribution transformer (DT) and ensuring a high power rate for the fast charging mode. In fact, the PV system is still inefficient and unstable in terms of power, due to the climatic changes in irradiation. However, this approach is still a research domain since many improvements have to be realized to optimize this combined charging supply.

The optimization approach used in this paper allows the power flow to drop properly between the PV/Battery and the grid. The battery storage buffer (BSB) is equipped with a battery management system (BMS) which controls the state of charge (SOC) [3], the time to full-load EVs is presented as an inconvenient constraint for the chargers. Moreover, for a highly performant autonomy of EVs, most forms of CS designs have the ability to respond to the loads demand, the National Household Travel Survey confirms that EVs are parked in workplaces for at least 5 hours [4]. In house places customers prefer charging at nighttime instead of day, which causes an overloading problem of the DT especially when the AC Load is also linked, indeed, the replacement of higher power rating transformers should be a solving choice. However, the power flow will

follow the instruction delivered by the energy management unit (EMU) of the CS. At this trend, data processing is treated in the EMU core to achieve and implement the appropriate power scenario for the CS, the target scenario is based on sensing the power state of the DC bus, besides, the continuity of service with a best power management is the main goal of this approach. Despite the overloading issue of the grid and the inefficiency of PV power, the use of BSB to substitute the PV&Grid may still an ultimate alternative for charging EVs when AC load is given high priority to connect with the utility and in the peak hours duration as well [5]. In this case, the balance between power demand and supply is the major purpose. Due to the fact that EV customers are tended to charge their batteries taking into consideration two constraint i.e. a short delay to plug and a low charging cost, in fact, there are three modes of charging EVs battery via the step-down choppers with current control to adapt the required plug-in mode of charge. Additionally, these type of converters offer a large margin of power due to the appropriate control system, each rated power correspond a specific charging mode [6], which are classified depending on charging time; Mode-1: Slow charging (used for domestic, long-time EV parking), Mode-2: Quick charging (used for private, public location), Mode-3: Fast charging (used for public location) [7]. Moreover, the reliance on renewable energies for electric vehicle charging station (EVCS) still needs improvements in many ways, especially for the fast charging mode.

2 Description of the EVCS Architecture

The PV system is connected to DC bus via DC/DC boost converter controlled by a MPPT algorithm that extracts maximum power from PV. The BSB is connected with DC bus via buck/boost converter, which adapts low voltage of the battery to the bus voltage [8]. Buck converters are used to charge EVs only through numerous modes of charge connected parallel to PV/BSB. Each charging points is contained a Human Control Panel (HCP) to insert information as the State of Charge (SOC) of the battery, duration time to load, the battery capacity and the power required to attend the desired SOC. Another specification is taken into account the company name/model of the vehicle to adapt properly the adequate mode of charge and determine the priority level to load when limited power is appears at the CS. The EMU performance of the EVCS diagram as shown the Fig. 1 is tested through many standards, for instance, extraction of maximum power from the panel which requires the appropriate algorithm and the switch between the modes of operation is also considered the main purpose of the controller [9]. Furthermore, the reference DC bus linked the multiple sources of energy has been chosen taking into consideration the switch operation and treats the HCP data provided by the EV user [10].

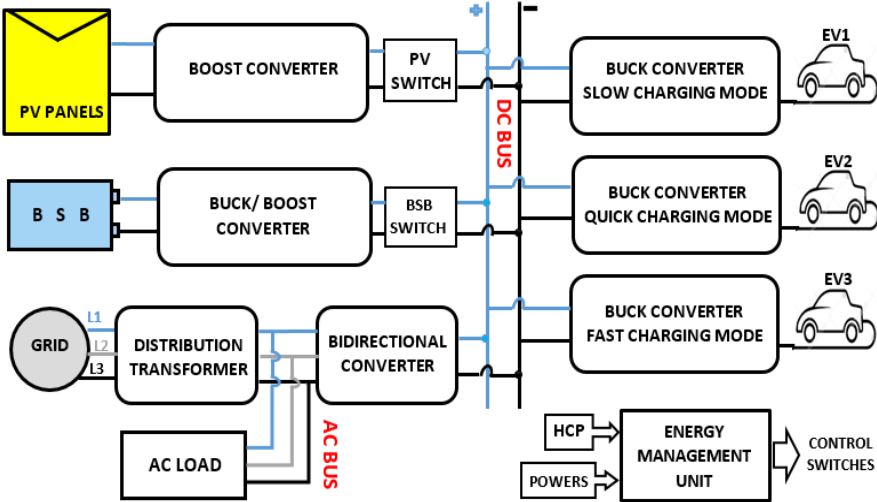


Figure1: Block diagram of different block of CS for EV

2.1 Photovoltaic Array

Solar photovoltaic cells may be designed with many different models [11]. This work uses the simplest and the significant equivalent circuit of a solar cell, it is made of a current source in parallel with a diode and a

shunt resistor. Fig. 2 illustrates the circuit diagram adopted in this project that will be translated to mathematical equations [12].

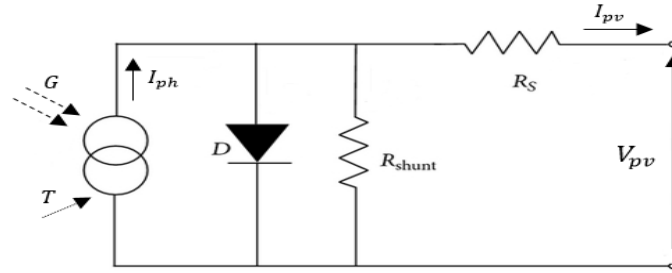


Figure2: Equivalent model of PV cell

The I_{pv} current delivered by the PV panel depends on multiple parameters as the solar cell series and parallel resistances R_s and R_{shunt} , the solar cell output voltage V_{PV} and the I_{ph} and I_s currents, all these parameters are described as follow:

$$I_{pv} = N_p I_{ph} - N_p I_o \left[e^{\frac{q(N_p V_{pv} + N_s R_s I_{pv})}{akTN_s N_p}} - 1 \right] - \frac{N_p V_{pv} + N_s R_s I_{pv}}{N_s R_{shunt}} \quad (1)$$

Where I_{ph} is the light generated current, I_o is the saturation current, q is the electron charge ($1.6 \times C$), a is the ideality factor (between 1 and 2), k is the Boltzmann constant ($1.38 \times J/K$), T is the cell temperature in Kelvin (K), N_s and N_p are the numbers of series and parallel cells respectively.

$$I_{ph} = [I_{ph,n} + K_i (T - T_{ref})] \frac{G}{G_n} \quad (2)$$

The I_{ph} current is linearly depend on the irradiance G (W/m^2) and the temperature of the junction, where T_{ref} is the reference cell temperature (298,15 K) and G_n is the nominal irradiance ($1000 W/m^2$), $I_{ph,n}$ is the light current generated at nominal conditions (T_{ref} et G_n), K_i is the current temperature coefficient [A/K].

$$I_o = I_{o,n} \left(\frac{T_{ref}}{T} \right)^3 \exp \left[\frac{q E_g}{a.k} \left(\frac{1}{T_{ref}} - \frac{1}{T} \right) \right] \quad (3)$$

The I_o current is affected by the variations of temperature, where $I_{o,n}$ is the nominal saturation current, V_{ocn} is the open circuit voltage, K_v is the voltage temperature coefficient [V/K] and E_g is the energy band gap (eV) [13].

$$I_{o,n} = \frac{I_{sc,n} + K_i (T - T_{ref})}{\exp \left(q \frac{V_{ocn} + K_v (T - T_{ref})}{a.k.N_s.T} \right)} \quad (4)$$

The use of MATLAB/Simulink interface provides the efficient simulation of the irradiance and the temperature variations, Fig. 3 describes the internal architecture of the PV generator using the previous equations for a mathematical modeling.

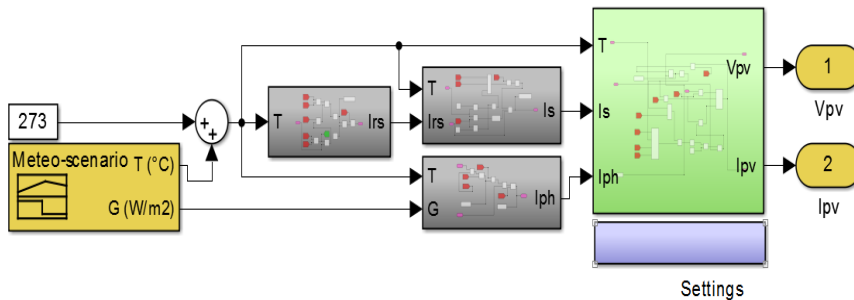


Figure3: Internal architecture of a photovoltaic generator

The PV panel has been modeled with mathematical units. The adjustment parameters block contains the nominal values i.e. atmospheric data and constants. However, Fig. 4 gathers all the electric blocks in one global pattern.

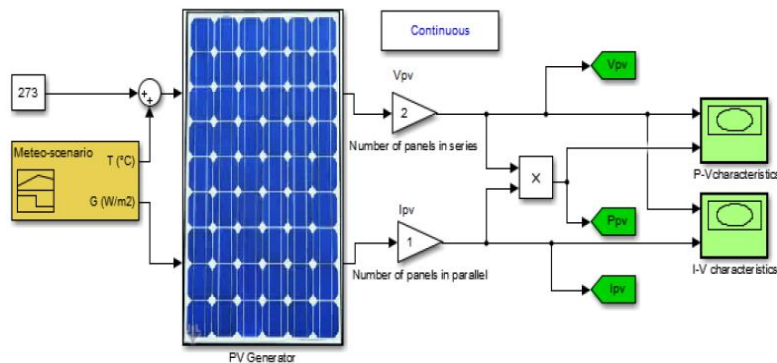


Figure4: Global design for a PV panels

The model of PV panel is designed carefully to simulate the ISF-240 array, it provides 240W of nominal maximum power, and has built with 60 monocrystalline silicon solar cells in series, *TABLE 1* shows the extra electrical specifications taken from the datasheet [14].

Table1: Electrical characteristics data of ISF-240 PV at 25 °C, 1kW/M2

Maximum Power (P_{max})	240 W
Maximum Power Voltage (V_{mpp})	30,3 V
Maximum Power Current (I_{mpp})	7,91 A
Open circuit voltage (V_{oc})	37,1 V
Short circuit current (I_{sc})	8,46 A
Voltage temperature coefficient (K_v)	-0,323 % / K
Current temperature coefficient (K_I)	0,042 % / K

The panel settings shown in *Tab. 1* are implemented in the settings block of the Fig. 3, N_{sp} and N_{pp} are referred to the number of panels connected in series and in parallel respectively, in this case, they are affected by a unit value. Thereby, all the experiments on the PV cells are done under the standard test conditions (STC). The values of the irradiance and the temperature in these conditions are; 25 °C, 1000 W/m². However, the simulation results of a PV panel examined under the STC is depicted in the Fig. 5. The current-voltage (I-V) characteristics and the power-voltage (P-V) characteristics reflect the simulation credibility of the PV panel data [15], the results are almost identical with the electrical data of the ISF-240 array panel.

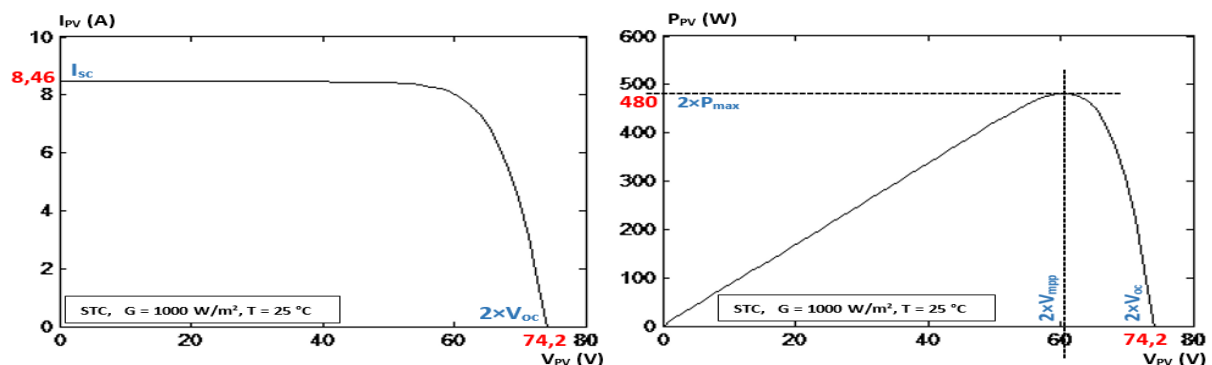


Figure5: Simulated I_{pv} - V_{pv} & P_{pv} - V_{pv} curves of ISF-240 PV (1KW/m², 25°C)

The Power-voltage characteristic has only one maximum power point called MPP and its position is continually changed because of the variation of irradiance and temperature, as is the case of the winter and the summer climate characteristics. Therefore, the simulation shows the same values and perspectives given by the datasheet.

2.2 DC/DC boost converter

2.2.1 Incremental Conductance algorithm

It might occasionally the panel output voltage does not reach the required value an account of the frequent variations of temperature and irradiance to which the panel is exposed, a reason that we use a converter to readjust the DC bus voltage despite the PV input variations. Furthermore, the dc-dc boost converter has been designed to maintain the DC bus voltage stable through an energy management unit (EMU) block. Although the generated duty cycle must secure some performance issues, as the extraction of maximum power from the PV panels using MPPT method, and ensure the long BSB lifetime during the charging phases.

The dc-dc boost converter load is representing the lithium-ion battery as a reference case. Moreover, the MPPT algorithm is implemented to extract maximum power from the PV, thus the Incremental Conductance (INC) algorithm is selected owing to its effectiveness, and to its fast response to detect the maximum power point [16]. The charging station controller unit requires the voltage control loop with PI to protect the battery from the overvoltage that MPPT is unable to handle it. Then the management algorithm chooses between the two methods depending on the circumstances of the PV power and the battery state of charge.

The electrical parameters of the boost converter are taking into account the delivered PV power through many specifications as the transistor frequency and the repeated oscillations of the input current and the output voltage of the converter. However, the CU block comprises a voltage control and MPPT algorithm using the Incremental Conductance (INC) method. The flowchart of the Fig. 6 describes the strategy of the MPPT applied to the power transistor.

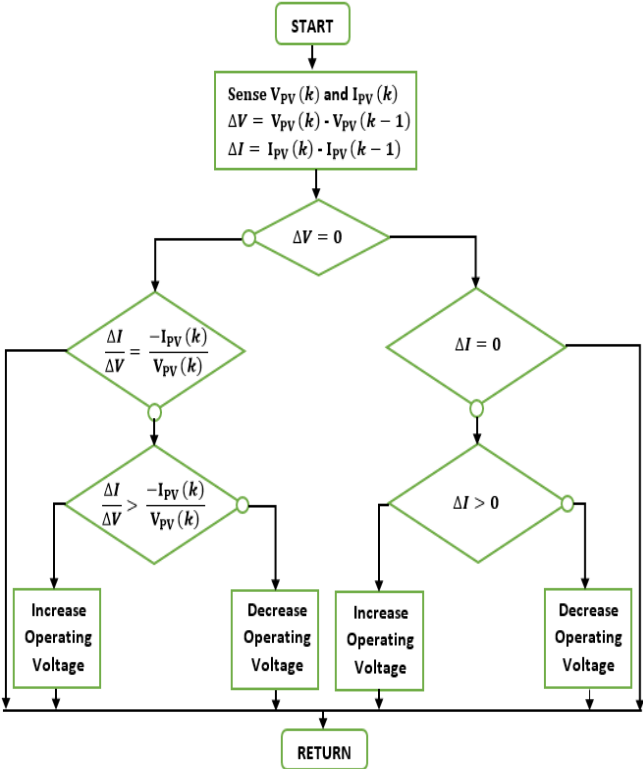


Figure6: Flowchart of the P&O MPPT method

Although recent literatures point that INC has a good compromise between performance and complexity of implementation. Thus the method is based on the two terms i.e. dP/dV and dI/dV , they are considered as dynamic indicators of tracking the MPP presented in the P-V curve and which direction is moving around it, meanwhile at the P_{max} range the PV panel operates when $dP/dV = 0$.

$$\frac{dP}{dV} = \frac{d(V.I)}{dV} = I + V \frac{dI}{dV} = 0 \quad (8)$$

If $dI/dV \cong \Delta I/\Delta V$ then (8) can be written as follow:

$$\frac{\Delta I}{\Delta V} = -\frac{I}{V} \quad (9)$$

When the (9) condition is reached the duty cycle should remain unchanged, means that it is operating in MPP, meanwhile, its voltage is matched the V_{mpp} .

2.2.2 Voltage current regulation loop

The main reason to implement the control loop is to avoid sudden degradation of battery performant, by mean of protecting it from a higher rate of current and voltage delivered by the PV system. Unlike generating gating pulses from MPPT algorithm, voltage and current control do not adapt the system at MPP, besides, there would be two kinds of voltage references that the control loop compares on of them to the measured voltage of the boost converter output [17]. However, the architecture is based on a cascaded control in voltage & current frame followed by PWM generator to send the duty cycle to the converter switch, the boost converter voltage is maintained constant at the voltage reference. The PI control parameters shall be chosen according to how much fast and stable the system reaction is required [18]. The major function of each PI block is detailed properly as shown Fig. 7.

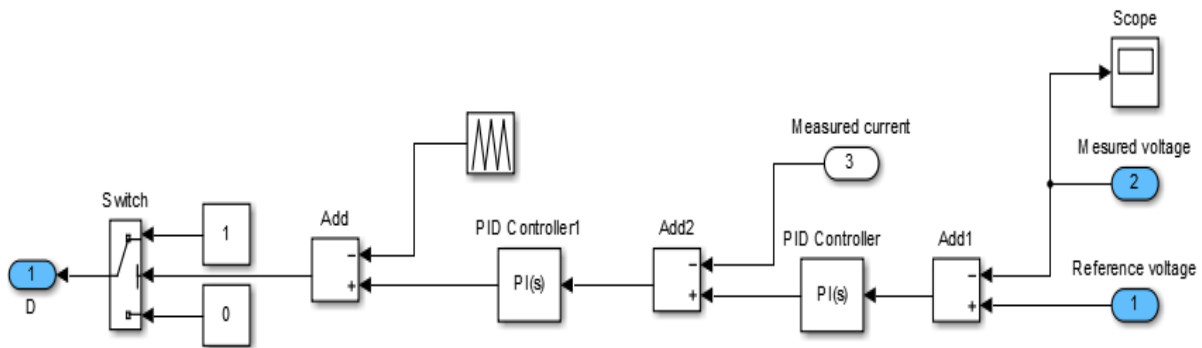


Figure7: Control loop block of voltage and current

The objective of defining the optimization problem is to benefit from a maximum range of MPPT mode duration, and quick switching unto the regulation voltage mode and reciprocally. Furthermore, the EMU treats its algorithm with a select control (CtrlS).

2.3 EV and battery storage buffer

The recent researches on storage battery technologies recommend the lithium-ion battery in the industrial market due to its high performance [19]. Economically speaking, more advantages of the use of lithium-ion battery are confirmed as the short return on investment (ROI) yield which affects the tendency of EV field [20]. Further, the integration of different energy sources in feeding the EV battery is shown in the Fig. 8.

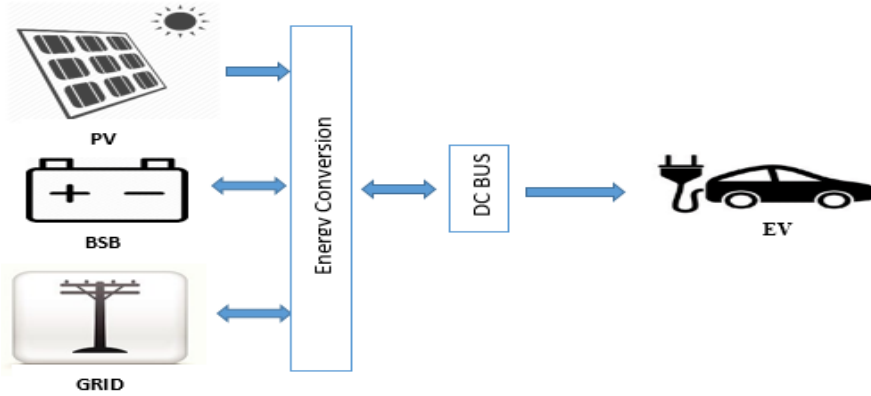


Figure8: Supply system for the EVB

The lithium-ion battery technology has become widely used in the highly performant storage system that required a specific characteristics e.g. fast charging, less self-discharge, working under wider operating temperature range and accepts higher recharge rate. The adopted battery is charged from two kinds of power i.e. the PV supply through the dc/dc converter and the grid, a reason to be controlled wisely to conserve its quality in the best conditions, as result, a long lifetime is ensured. Moreover, the electrical behaviour of the battery is expressed via three different phases illustrated in the Fig. 9. Each state has been handled using a convenient sort of control i.e. MPPT algorithm, voltage loop control.

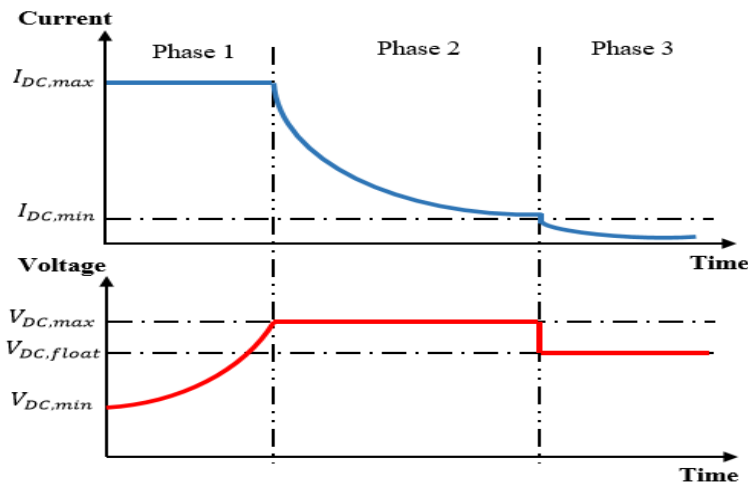


Figure9: BSB charging phases

The BSB battery first phase is controlled using the adopted MPPT method by dint of the safety margin of the DC bus voltage which is betwixt the allowed minimum value V_{DCmin} and the overload maximum value V_{DCmax} , meanwhile the DC bus current is fixed to the maximum I_{DCmax} to avoid overheating and overstrain phenomena. Once V_{DC} achieve V_{DCmax} , means the battery is actually operating in the second phase where the EMU is switching off the MPPT algorithm and adjusting the voltage control to the V_{DCmax} value. Nevertheless, the value of I_{DC} is kept increasing until it falls under I_{DCmin} where the third phase is reached, and in response the EMU rehabilitate the control voltage to a reduced value V_{Ref} , this reference voltage is able to avoid the deep self-discharge of the battery by generating a very small charging current [21].

2.4 Energy management unit

The EMU procedure contains the control of power flow between the two streams, and it rules the switches, besides, multiple dynamic inputs are made the adopted management algorithm more complex and performant as well. Yet, the extraction of maximum power from the PV array is recognized as the first task of the unit, which generates the matched duty cycle of the MPP for the dc-dc boost converter, the voltage and current loop control is also taken into consideration using the knowledge of I_{DC} and V_{DC} values. Moreover, the

maximum current delivered by the grid utility is taking into account the power consumed by both, the AC load and the CS with batteries, based on this fact, the limited current of the distribution transformer must be determined. A battery management system is implemented in the EMU when the BSB is fully charged and in the deep of discharge (DoD) circumstances. In terms of reliability, and to maintain a long lifetime for the batteries, their depth of discharge rate should be limited to 15-85 % [22].

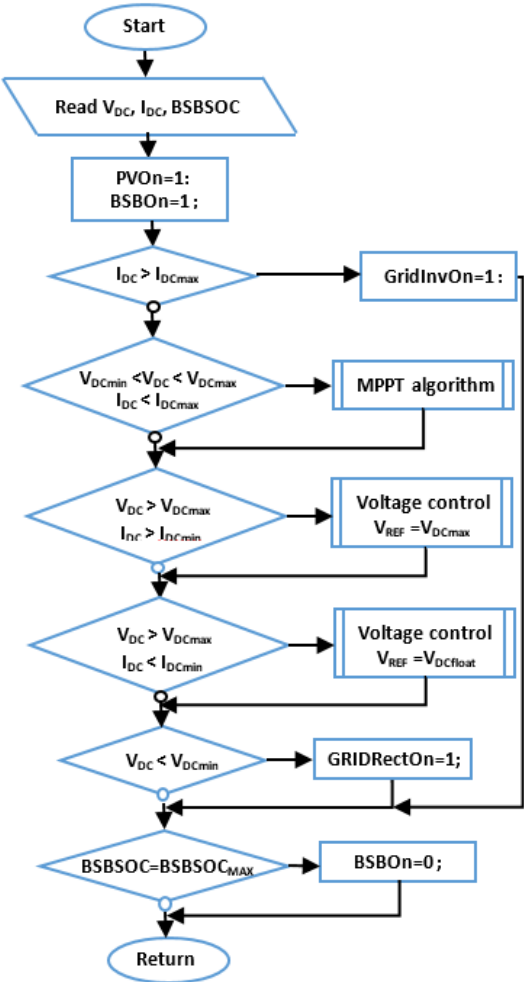


Figure10: Flowchart of the energy management approach

The adopted flowchart of the Fig. 10 shows the proposed strategy of energy management at the DC bus, the algorithm requires the continuous knowledge state of BSB settings e.g. the maximum average of V_{DC} , I_{DC} . Actually, the measurement of current and voltage of the DC bus and the SOC of BSB are the main keys to decide the power flow direction. The grid utility is chosen via two switches as the case of GridRecOn for a rectifying operation mode (Grid to CS), and the injection of extra power through the GridInvOn switch (CS to Grid). However, the storage battery is equipped with a management system to protect it from the deep discharge and when a full charge is attended, besides, the BSBO switch purpose is to secure the best lifetime for the CS batteries. Call program of MPPT algorithm is used in ordinary cases, when the output voltage across the limited voltage of BSB, therefore, the EMU will switch to the voltage control method to preserve the battery performance.

The utilization of Matlab/Simulink software provides the simplest perspective of strategy of the energy management control, the environment capability is the ability to simulate multiple parameters in an efficient structure. Otherwise, the PV current and voltage are considered main inputs for the EMU, the unit generates the suitable duty cycle for the dc/dc converter. Additionally, the DC link characteristics are also the keys to

this strategy with the SOC of the CS batteries. Fig. 11 illustrates the proposed EMU, which the outputs are impulses to all power switches, such as PVOn, BSBOn, GridRecOn and GridInvOn [23].

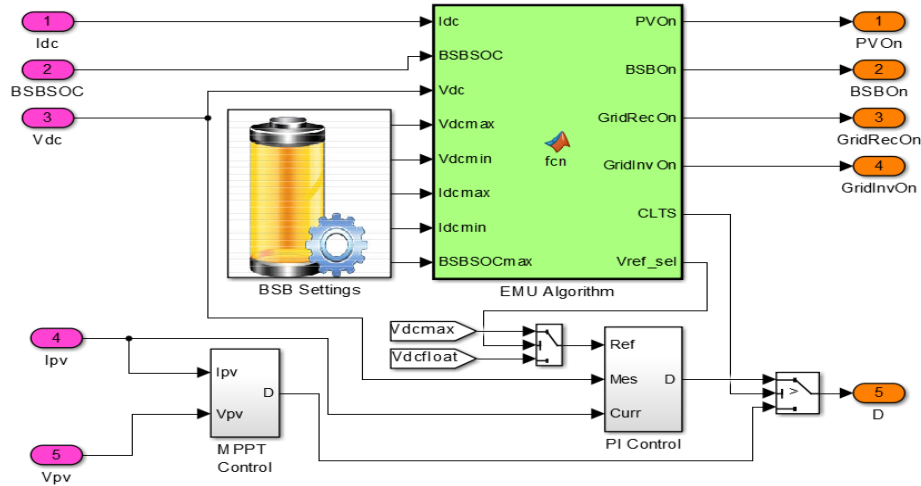


Figure 11: Internal diagram of energy management unit of the PV-Grid system

3 Simulation results

The validation test of the proposed topology is designed through a PV system prototype, which contains two panels mounted in series delivering 480 Wp. The MPPT algorithm and the voltage current control loop are implemented in the DC boost converter following the flowchart designations of the power flow. Moreover, the DC bus voltage is adapted at 400 V due to the various sources like the BSB of 48 V/8.3 Ah, which is tied to the DC bus through a buck/boost converter. The distribution transformer is also combined using a bi-directional AC/DC converter. However, Fig. 12 shows the designed structure including both the power and the control part, the EMU controls the SOC of the batteries, manages the fluctuation of power at the DC bus level, and operates each switch of the PVGS.

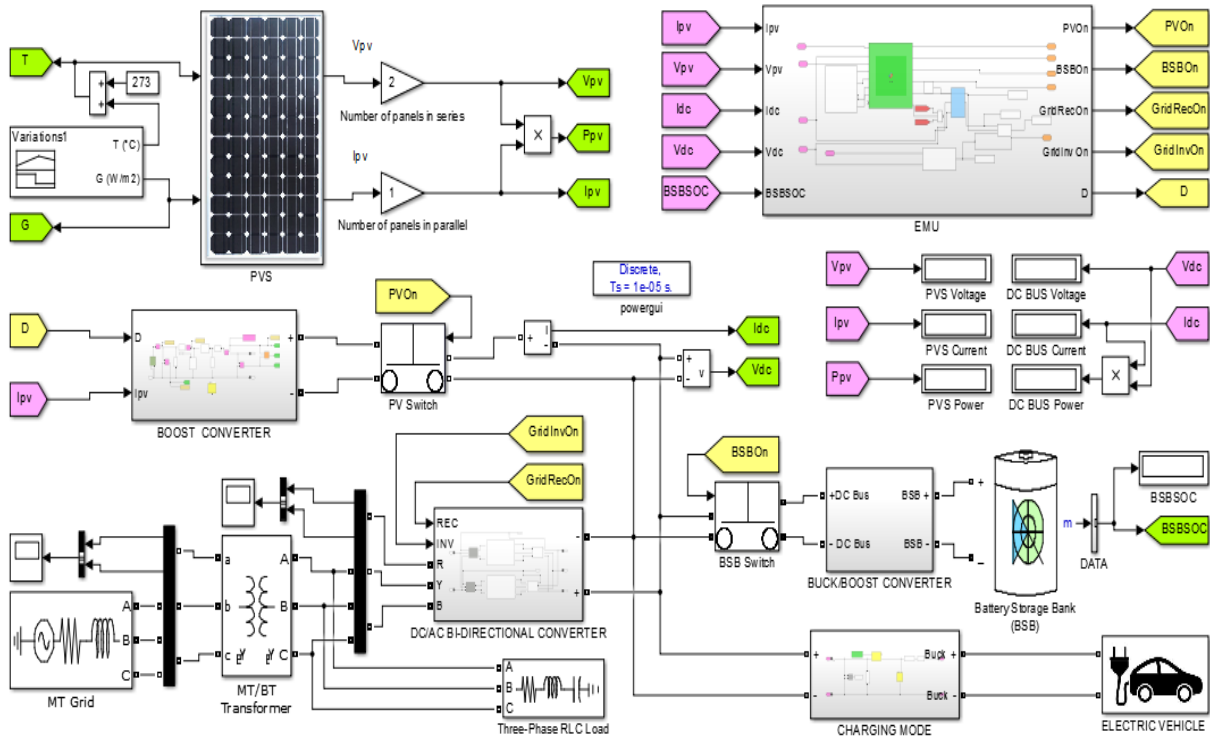


Figure 12: PV-Grid system for the charging station battery

The PV system is working with MPPT algorithm in order to generate the maximum available power from a low value of sun irradiance, besides, for reasons of energy optimization and ensure the best lifetime of the batteries, a voltage control loop is also included in the boost converter. The system is able to operate under a few scenarios. Fig. 13 depicts a climatic scenario implemented in the PVGS, which represents an actual case of climatic condition.

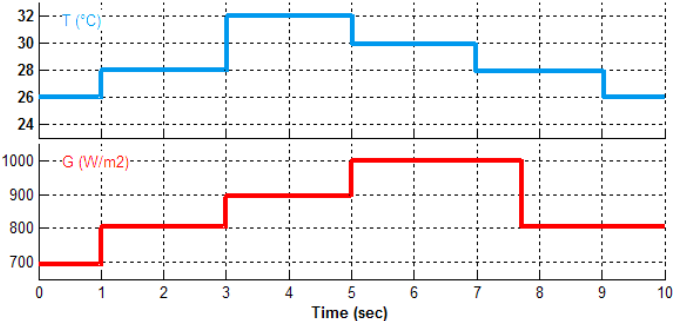


Figure13: Meteorological scenario of solar irradiation and temperature

The DC link voltage and current are shown in Fig. 14. As can be seen, the boost converter raises the PV voltage to a specific voltage margin (min; max), where the EMU operates under different modes, for instance; PV-standalone mode and the bidirectional power flow of the CS with utility grid. Basically, the irradiance scenario has determined the current flow provided by the PV array.

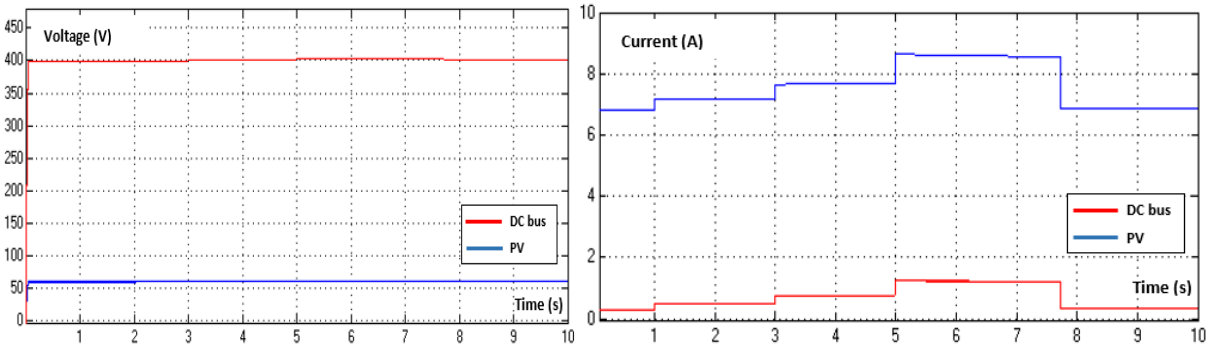


Figure14: DC bus voltage and current of the system versus time

To show the real performance of the EMU for voltage sustaining of the DC bus, the results obtained from the two kinds of control strategy of the boost converter have been plotted via simulation test of the proposed climatic scenario. In the meanwhile, the system reaches the steady state in short delay with a small margin of error due to the PI controller, another outcome is to reduce the large perturbation in DC bus voltage and to gain the maximum power with MPPT. The Fig. 15 shows the power state of charging BSB via PV system.

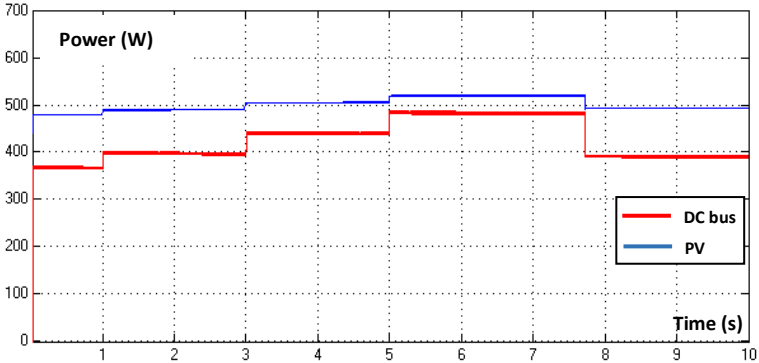


Figure15: Charging station DC power versus time

By means of testing the contribution of the electricity network, Fig. 16 depicts the similarity of energy between the PV system and the grid, where the BSBOn, PVOn and GridRecOn are activated.

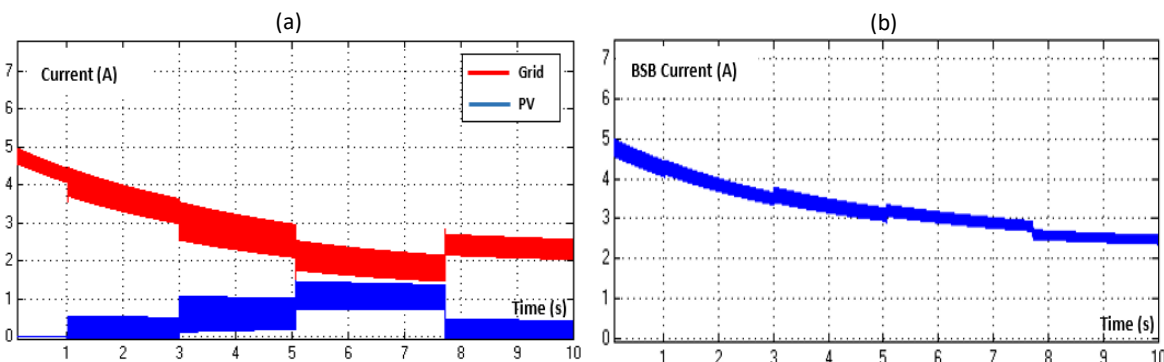


Figure16: Charging currents versus time (a) Grid/PV current (b) BSB charging mode

The curve (a) shows the charging process of the BSB through two kinds of energy sources, the phenomenon of complementarity in decreasing mode of current is illustrated in (b).

Conclusion

In this work, a smart topology of EVCS has been described with multiple optimization methods, simulation results confirmed the validity of the proposed control strategy. At this trend, the combination of two kinds of control for the converters made the management algorithm capable of implementing the appropriate power flow scenario. However, following the generated instructions from the EMU, its algorithm aimed to establish an intelligent compromise between the different sources of energy including the reaction of the electricity network, with the BSB support the CS is now able to ensure various charging modes to feed an EV battery under difficult circumstances. Besides, the AC load is also considered an inconvenient concern for the power stability at the DC link. To test the CS performance, climatic scenarios are implemented with the variations of temperature and irradiance, where PV system is in inefficiency state.

References

- [1] P. Grahn and L. Söder, "The customer perspective of the electric vehicles role on the electricity market," *2011 8th Int. Conf. Eur. Energy Mark. EEM 11*, no. May, pp. 141–148, 2011.
- [2] F. A. V Pinto, L. H. M. K. Costa, and M. Dias De Amorini, "Modeling spare capacity reuse in EV charging stations based on the Li-ion battery profile," *2014 Int. Conf. Connect. Veh. Expo, ICCVE 2014 - Proc.*, pp. 92–98, 2015.
- [3] K. Vitols, "Lithium ion battery parameter evaluation for battery management system," *RTUCON*, pp. 7–10, 2015.
- [4] A. Santos, N. McGuckin, H. Y. Nakamoto, D. Gray, and S. Liss, "Summary of travel trends: 2009 national household travel survey," 2011.
- [5] F. Locment, M. Sechilariu, and C. Forgez, "Electric vehicle charging system with PV Grid-connected configuration," *2010 IEEE Veh. Power Propuls. Conf.*, pp. 1–6, 2010.
- [6] J. P. Torreglosa, P. García-Triviño, L. M. Fernández-Ramirez, and F. Jurado, "Decentralized energy management strategy based on predictive controllers for a medium voltage direct current photovoltaic electric vehicle charging station," *Energy Convers. Manag.*, vol. 108, pp. 1–13, 2016.
- [7] G. R. C. Mouli, P. Bauer, and M. Zeman, "Comparison of System Architecture and Converter Topology for a Solar Powered Electric Vehicle Charging Station," pp. 1908–1915, 2015.
- [8] T. Sriboon, S. Sangsritorn, P. G. Tuohy, and M. K. Sharma, "Simulation and Analysis of Renewable Energy Resource Integration for Electric Vehicle Charging Stations in Thailand," no. September, pp. 14–16, 2016.

- [9] P. Goli and W. Shireen, "PV powered smart charging station for PHEVs," *Renew. Energy*, vol. 66, pp. 280–287, 2014.
- [10] T. Kamal, M. Nadarajah, S. Z. Hassan, H. Li, F. Mehmood, and I. Hussain, "Optimal Scheduling of PHEVs in a PV based Charging Station," pp. 1–6.
- [11] B. Fatiha, M. Th, C. Photovolta, and C. Mincez, "Study and optimization of the operation of a photovoltaic system," pp. 1–93, 2013.
- [12] S. Sumathi, L. Ashok Kumar and P. Surekha, *Solar PV and Wind Energy Conversion Systems*, ISBN 978-3-319-14940-0, 978-3-319-14941-7, 2015.
- [13] D. ABBES, "Contribution sizing and optimization of wind-solar hybrid systems with batteries for autonomous habitat residentia," 2006.
- [14] "ISF-240 Data sheet," ISOFOTON, Málaga, Spain.
- [15] A. . Fallis, "Modeling PV system," *J. Chem. Inf. Model.*, vol. 53, no. 9, pp. 1689–1699, 2013.
- [16] D. Sera, T. Kerekes, R. Teodorescu, and F. Blaabjerg, "improved Environmental Conditions," pp. 1614–1619, 2006.
- [17] N. Carrero, C. Batlle, and E. Fossas, "Experimental evaluation of a cascade sliding mode-PI controller for a coupled-inductor Boost converter," *Proc. IEEE Work. Appl. Comput. Vis.*, vol. 0, no. 1, pp. 1–6, 2014.
- [18] B. Panda, A. Sarkar, B. Panda, and P. K. Hota, "A Comparative Study of PI and Fuzzy Controllers for Solar Powered DC-DC Boost Converter," *2015 Int. Conf. Comput. Intell. Networks*, pp. 47–51, 2015.
- [19] D. Antonio, B. Di, and E. Bocci, "Energy analysis of a real grid connected lithium battery energy storage system," *Energy Procedia*, vol. 75, pp. 1881–1887, 2015.
- [20] M. Naumann, R. C. Karl, C. N. Truong, A. Jossen, and H. C. Hesse, "Lithium-ion battery cost analysis in PV-household application," *Energy Procedia*, vol. 73, pp. 37–47, 2015.
- [21] J. López, S. I. S. Jr, P. F. Donoso, L. M. F. Morais, P. C. Cortizo, and M. A. Severo, "Digital control strategy for a buck converter operating as a battery charger for stand-alone photovoltaic systems q," vol. 140, pp. 171–187, 2016.
- [22] M. O. Badawy, "Power Flow Management of a Grid Tied PV-Battery Powered Fast Electric Vehicle Charging Station," pp. 4959–4966, 2015.
- [23] A. Hassoune, M. Khafallah, A. Mesbahi, and D. Breuil, "Electrical design of a photovoltaic-grid system for electric vehicles charging station," pp. 228–233.



Abdelilah Hassoune was born in Settat, Morocco in 1993. He received the bachelor diploma in mathematical sciences in 2010, and the technical university degree in electrical engineering and computer science from the National High School of Technical Education, Mohammedia, Morocco, in 2012, and the master degrees from the Multidisciplinary Faculty of the Hassan I University, Khouribga, Morocco, in 2013, and the electrical engineer diploma in embedded systems and numerical control from the National School of Applied Sciences Khouribga, Morocco, 2015. He joined the Hassan II University of Casablanca, ENSEM, Morocco, in 2015 as a PhD candidate at the Laboratory of Energy & Electrical Systems. His research interests include electric vehicles charging station.